Applied Environmental Research
- RESEARCH FOR SUSTAINABLE PLANET -

Research Article

Alstonia Scholaris Fruit Biomass, a Novel Adsorbent for the Removal of Lead from Aqueous Solution

Aasif Abdullah Baba, Ajit Kumar Dasa*, Abhik Gupta

Department of Ecology & Environmental Science, Assam University, Silchar -788011, Assam, India

*Correspondence Email: ajit.kumar.das@aus.ac.in

Abstract

The biosorption of lead (Pb) ions on *Alstonia scholaris* fruit biomass was investigated in batch and column experiments in an aqueous solution, emphasising the possible binding mechanism of Pb ions on the fruit biomass. The adsorption process was found to be dependent on parameters like adsorbent dose, initial Pb ion concentration, contact time, and pH. No impact was found on Pb adsorption during competitive adsorption. The results suggested that the fruit biomass could remove more than 97% of Pb ions from the aqueous solution. The Freundlich isotherm model best explained the obtained results. The monolayer adsorption capacity of the *A. scholaris* fruit biomass was 50 mg g^{-1}. The reaction rate was fast initially with most Pb adsorption taking place during the first 80 minutes, while the equilibrium was attained at 420 minutes. Scanning electron microscopy revealed changes in the surface texture of *A. scholaris* fruit biomass after adsorption of Pb. The biomass's surface area was determined using Brunauer-Emmett-Teller technique. Desorption, Fourier transform infrared spectroscopy, and functional group modification revealed that the bonding of Pb ions on *Alstonia scholaris* fruit biomass involved complex mechanisms.

ARTICLE HISTORY

Received: 31 Oct. 2023
Accepted: 28 May 2024
Published: 27 Jun. 2024

KEYWORDS

Biosorption;
Alstonia scholaris;
Desorption;
Modification;
Binding;
Complexation

Introduction

Heavy metal contamination of both natural and artificial ecosystems is a global issue of concern. Among the various heavy metals, lead (Pb) is considered an important toxic contaminant of the environment with grave implications for public health. Manufacturing industries, such as batteries, electronics, and others, are the primary sources of Pb contamination of the environment. Pb has a disastrous impact on human health even at low concentrations, causing nervous and reproductive failure, kidney and brain failure, vomiting, and cramps. Thus, mitigating Pb pollution is a high priority goal for protecting aquatic and terrestrial life [1–2].

Pb and other heavy metal contamination of water and wastewater can be removed or reduced with the help of different physicochemical and biological techniques, which include electrochemical treatment, membrane processing, and flotation, among others. However, these methods have certain drawbacks, such as toxic sludge generation, ineffectiveness at lower ambient concentrations of metals, and high cost. Consequently, developing cost effective and cheap adsorbents is critical to the treatment of metal-contaminated water [3].

Adsorption is considered a promising as well as cost-effective and eco-friendly technology for removal of metal ions from contaminated water. It is, therefore, necessary to find efficient and easily available adsorbent biomaterials from plants and microorganisms. Biosorption has some merits over the conventional methods, such as the absence of toxic sludge, potential reuse of the bioadsorbent, and reduction of heavy metal pollution to less harmful levels [4].

Biosorption is a passive process; it does not require metabolic energy to bond the metal ion on dead biomass. The adsorption mechanism is not well understood but

https://doi.org/10.35762/AER.2024030

depends on the adsorbent type and the adsorbate metal.

Biosorption can be explained by the biomaterial capacity to adsorb or extract toxic heavy metals from metal-contaminated water with physical and chemical procedures. The ability of an adsorbent to remove heavy metals, and its correlation with different techniques must be first analysed before developing it as an adsorbent of industrial calibre. Different biomasses such as bacterial, fungal, algal, industrial waste and agricultural waste biomass are used as adsorbents. Agricultural wastes are highly suitable because these are less costly and mostly find no other use. For example, the Pb adsorption capacities of waste tea leaves, banana peel, rice bran, wheat straw, cassava peel, Picea smithiana sawdust, and yam peel were 73, 45.6, 416.61, 599.1, 5.80, 6.35, and 98.36 mg g^{-1}, respectively [5–6]. From the above discussion it can be concluded that the adsorbents prepared from agricultural and plant based waste have potential to adsorb Pb from the wastewater. Keeping in view this property of these waste-based adsorbents, in the present article we investigated the removal of Pb with biomass obtained from the fruit body of Alstonia scholaris plant through adsorption technique. This plant was selected because it has not been studied as an adsorbent for the Pb removal from the aqueous solutions and the material obtained is considered as an agricultural waste. It is either burned or disposed as it is and is abundantly available at low cost. In addition to this the adsorbent prepared was free from any chemical, thus environment friendly. The aim of the study is to identify a new cost-effective, environment friendly bioadsorbent by demonstrating its adsorption efficiency for the Pb ion in a single metal and multimetal solution. The present study took into account several parameters such as adsorbent dose, initial Pb ion concentration, pH, rotation per minute, and contact time using the batch method. Desorption and chemical treatment were done to analyse the regeneration capacity of the adsorbent and mechanism of sorption. Isotherms and kinetic parameters were deducted from adsorption experiments. Scanning electron microscopy (SEM) was used to study the surface morphology of the ASF adsorbent, and the surface area of the adsorbent was studied through Brunauer-Emmett-Teller (BET) analysis [7].

Materials and methods

1) Preparation of biomass

Alstonia scholaris fruit (ASF) body was collected from the Silcurie (24.724838°N, 92.782596°E) area of Cachar district, Assam, India. The fruit body was cut, washed with tap water, followed by washing with distilled water to remove impurities from the material. It was then oven dried at 50 °C for 24 h, ground to powder, sieved at 1 μm, and again oven dried at 50 °C to constant weight.

2) Metal stock solutions

Lead nitrate, Cadmium chloride, Cupric chloride and Zinc chloride of analytical grade were used to prepare the stock solutions for the experiments. The concentration of the stock solutions was 1,000 mg L^{-1}, which were diluted to get the desired Pb, Cd, Cu, and Zn concentrations.

3) Characterisation of the adsorbent

The surface area of the ASF biomass was determined by nitrogen adsorption at -196 °C by a surface area analyser (Model No. Tristar II; Make: M/s Micromeritics, U.S. A). The sample was degassed under vacuum at 50 °C. The morphology of ASF biomass was analysed in a scanning electron microscope (JEOL, JAPAN; Model: JSM 6390LV) after mounting the biomass samples on stubs coated with a thin layer of gold. The SEM micrographs were taken at an accelerating voltage of 20kV. The functional group of ASF biomass was investigated in a Fourier transform infrared spectrometer (NICOLET, USA; Model: IMPACT 410) over a wave-number range from 4,000 to 400 cm^{-1}.

4) Adsorption experiment

The experiment was done in batch mode. An array of 250 mL Erlenmeyer flasks containing 100 mL of Pb-nitrate solution was put on the shaker. To determine the impact of a given variable such as agitation speed (0–230 rpm), adsorbent dose (0.5–5 g), pH (3–10), initial Pb ion concentration 43.21–431.02 mg L^{-1}, and contact time (80–1680 min), only that particular variable was altered, keeping all the others constant. The equilibrium adsorption isotherm was studied at measured Pb ion concentrations of 43.21 mg L^{-1} – 431.02 mg L^{-1}. The adsorption kinetics of Pb by ASF biomass was conducted up to 420 min at Pb ion concentrations of 81.27 mg L^{-1} and 198.78 mg L^{-1}. The concentrations of Pb, Cd, Cu, and Zn were analysed in the test water used for the adsorption study before commencing the adsorption experiments in order to determine the actual initial concentrations of these metals. The concentrations of these metal ions before and after the adsorption experiment were determined by ICP-AES (ARCOS, Simultaneous ICP Spectrometer, SPECTRO Analytical Instruments GmbH, Germany). Experiments were carried out in triplicates as a standard procedure.

5) Chemical modification of the biomass

The *A. scholaris* fruit biomass was subjected to chemical treatment in order to modify its properties which was then used in adsorption experiment to remove lead, the modification was done as follows:

Modification of carboxylic groups: 5 g of ASF biomass and 65 mL of anhydrous methanol were mixed, and 0.6 mL of hydrochloric acid was added to the solution. The solution was put on a shaker for 6 h at 170 rpm [8].

Modification of amine group: 5 g of ASF biomass was added to 40 mL of formic acid and 20 mL of formaldehyde. The solution was put on a shaker for 6 h [9].

Modification of lipids: 5 g of ASF biomass was added to 50 mL of acetone. The mixture was heated under reflux for 2.5 h [10].

6) Desorption Experiment

Desorption experiments were also performed in batch mode. Four different desorption eluents: H_2O (deionised), NaOH (0.1M) [11], HNO_3 (0.1M) [12], and EDTA (0.1M) [12] were used. ASF biomass from adsorption experiments was used in these desorption experiments, and used ASF biomass was immersed in 100 mL of desorption eluent in 250 mL Erlenmeyer flasks. Adsorbent-desorption liquid was agitated at 150–160 rpm for 1 h. Relation between time and desorption with H_2O was also investigated by varying time from 1–24 h.

7) Estimation of metal

The proportion of metal ions adsorbed per unit ASF adsorbent mg g^{-1} and adsorption efficiency was estimated by adopting Eq. 1 and 2 respectively, [13]:

$$q_e = \left[\frac{C_o - C_e}{M}\right] v \qquad \text{(Eq. 1)}$$

$$\text{Adsorption}(\%) = \frac{C_o - C_e}{C_o} \times 100 \qquad \text{(Eq. 2)}$$

Where q_e is the proportion of Pb metal ions adsorbed on biomass (mg g^{-1}), Co is the initial metal ion concentration in the solution (mg L^{-1}), Ce is the equilibrium metal ion concentration of the solution (mg L^{-1}), v is the solution volume (L), and M denotes the mass of ASF biomass added to the solution (g).

8) Adsorption isotherms

In the present research, the following isotherm equations were applied to experimental data: Langmuir (Eq. 3–4), Freundlich (Eq. 5–6), Temkin Isotherm (Eq. 7), and Dubinin-Radushkevich (D-R) Isotherm (Eq. 8):

$$q_e = \frac{q_m K_L C_e}{1 + K_L C_e} \qquad \text{(Eq. 3)}$$

Linear form of Langmuir isotherm is shown in Eq. 4 [14]:

$$\frac{C_e}{q_e} = \frac{1}{K_L q_m} + \frac{C_e}{q_m} \qquad \text{(Eq. 4)}$$

$$q_e = K_F C^{1/n} \qquad \text{(Eq. 5)}$$

The linear Freundlich equation is shown in Eq. 6 [15]:

$$\log q_e = \log K_F + \frac{1}{n} \log C_e \qquad \text{(Eq. 6)}$$

The equilibrium Pb ion concentration is Ce (mg L^{-1}), the Langmuir adsorption capacity is q_m (mg g^{-1}), and the metal adsorbed on the biomass is q_e (mg g^{-1}). The Langmuir and Freundlich isotherm constants are K_L and K_F (Lg^{-1}), respectively, and the heterogeneity factor is 1/n.

$$q_e = \frac{RT}{b} ln K_T + \frac{RT}{b} ln C_e \qquad \text{(Eq. 7)}$$

Where, Temkin constant is b (J mol^{-1}) and Temkin Isotherm constant K_T (Lg^{-1}) [16].

The equation of D-R isotherm is shown in Eq. 8 [17]:

$$ln q_e = ln q_m - \beta\varepsilon^2 \qquad \text{(Eq. 8)}$$

$$\varepsilon = RT ln\left(1 + \frac{1}{C_e}\right) \qquad \text{(Eq. 9)}$$

$$E = 1/\sqrt{2B} \qquad \text{(Eq. 10)}$$

Where ε is Polanyi potential, β is D-R constant, R is gas constant (8.31 J mol^{-1} k^{-1}), T is the absolute temperature, and E is mean adsorption energy. This model distinguishes between the physical and chemical adsorption on the basis of free energy.

To understand the adsorption data efficiently, Scatchard (Eq. 11) analysis was performed [18].

$$q/C = q_m K_b - q K_b \qquad \text{(Eq. 11)}$$

The equilibrium adsorption capacity is determined by q, while the equilibrium Pb ion concentration is determined by C. The adsorption isotherm constants are determined by q_m and K_b.

9) Kinetic studies

Kinetic studies were done using several linear and non-linear models. In the present study, the data obtained were investigated adopting pseudo-first-order (Eq. 12–13), pseudo-second-order (Eq. 14–15) and intraparticle diffusion (Equations 16 and 17) models [19].

$$q_t = (q_e - e - K_1 t) \quad \text{(Eq. 12)}$$

$$log(q_e - q_t) = log q_e - \frac{K_1}{2.303} t \quad \text{(Eq. 13)}$$

$$q_t = \frac{K_2 {q_e}^2 t}{1 + K_2 {q_e}^2 t} \quad \text{(Eq. 14)}$$

$$\frac{t}{q_t} = \frac{1}{K_2 q_e^2} + \frac{1}{q_e} t \quad \text{(Eq. 15)}$$

The amount of Pb adsorbed at equilibrium is q_e (mg g^{-1}) and the amount of Pb ions adsorbed at a time 't' is q_t (mg g^{-1}). The first and second order rate constants are K_1 and K_2 respectively.

To analyse the potential impact of intraparticle diffusion on Pb adsorption, the intraparticular diffusion model was used.

$$q_t = K_p t^{1/2} + C \quad \text{(Eq. 16)}$$

The intraparticular diffusion rate constant is K_p (mg g^{-1} $min^{-1/2}$), while the intercept is C (mg g^{-1}).

10) Error analysis

Error analysis was performed using the following error functions (Eq. 17–20).

Results and discussion

1) Impact of pH, adsorbent dose, contact time, initial Pb concentration, and agitation speed

The pH is a crucial factor in adsorption experiments and significantly impacts the adsorption efficiency of adsorbents. As depicted in Figure 1(a), the maximum adsorption (91.31%) of Pb took place at pH 5. When the pH was increased from 3.0 to 5.0, the adsorbent surface became negatively charged, facilitating ion binding on the adsorbent, while above pH 5, reduction in adsorption was due to the precipitation of metal complexes [23].

Biomass loading is an essential factor for bio-adsorbent efficiency. Figure 1(b) shows the adsorption efficiency of ASF biomass for Pb ions as a function of adsorbent loading. ASF adsorbent exhibited improved sorption efficiency up to 2.50 g per 100 mL beyond which adsorption decreased. The observations can be explained by the fact that a lower adsorbent dose in solution corresponds to a lesser number of active binding sites and decrease in adsorption efficiency can be attributed to the aggregate formation by adsorbent particles [24]. In our study, the highest Pb adsorption of 97.25% was achieved at an adsorbent dose of 2.50 g per 100 mL.

Contact time is the most influential parameter in the sorption process. Figure 1(c) shows the impact of contact time on the binding of Pb ions on ASF biomass. The peak adsorption efficiency of ASF biomass reached at 420 min (95.58%) potentially due to unoccupied active binding sites with the passage of time, the rate gradually decreased because of the growing unavailability of active binding sites. Contact time has been demonstrated to have a similar effect on Pb adsorption with copper oxide nanostructures [25].

Root mean square error (RMSE): $\sqrt{\frac{1}{n-2}\sum_{i=1}^{N} q_{e(exp)} - q_{e(cal)}}$ (Eq. 17)

The chi-square test: $X^2 = \sum_{i=1}^{N} \frac{q_{e(exp)} - q_{e(cal)})^2}{q_{e(cal)}}$ (Eq. 18)

The sum of absolute error (EABS): $\sum_{i=1}^{N} (q_{e(exp)} - q_{e(cal)})$ (Eq. 19)

Standard Deviation (SD) = $\sqrt{\frac{1}{N-P}\sum_{i=1}^{N} (q_{e(exp)} - q_{e(cal)})^2}$ (Eq. 20)

Where $q_{e(exp)}$ is the observed value, $q_{e(cal)}$ is the value predicted by the models, and N represents the data points [20–22].

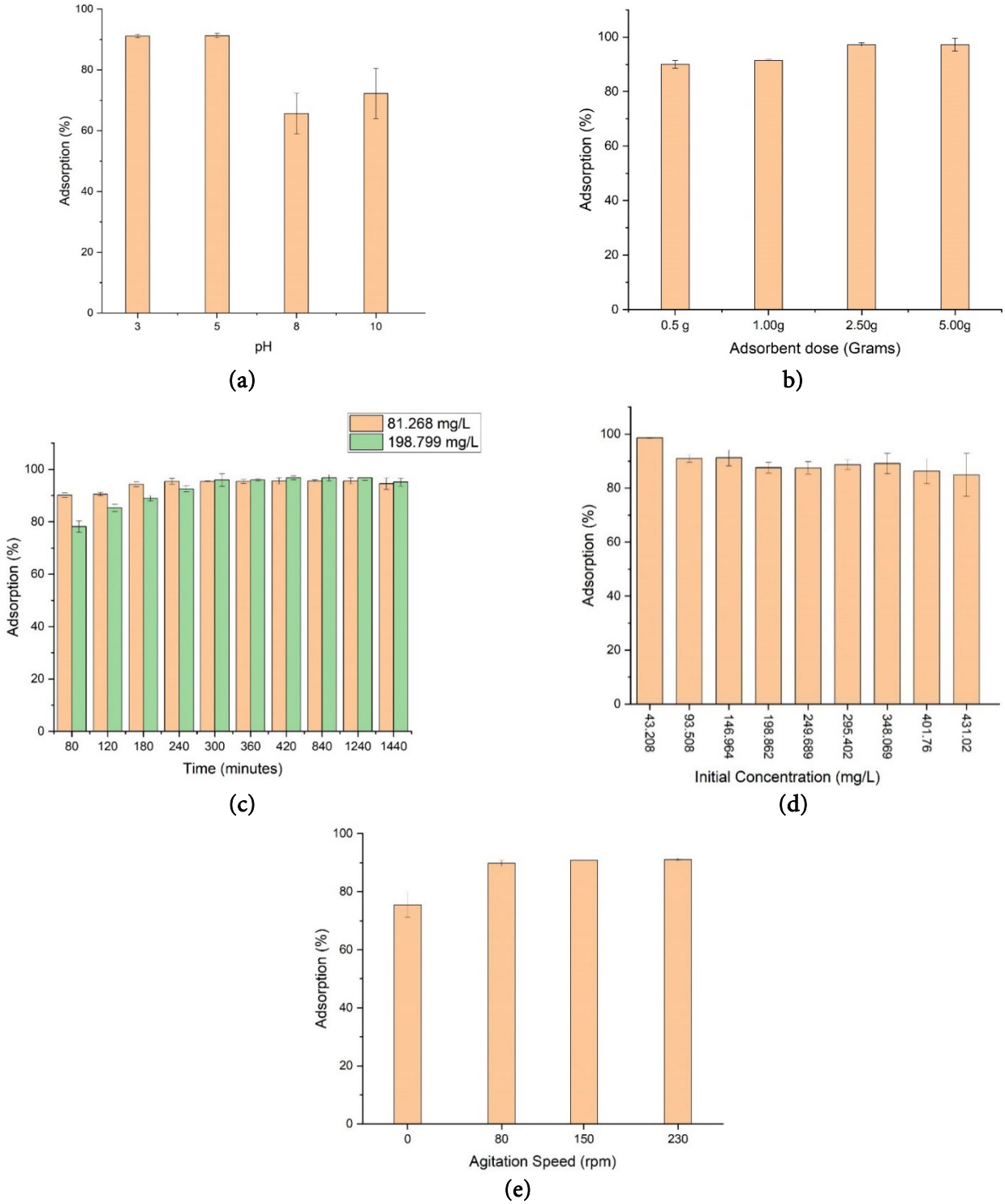

Figure 1 Impacts of (a) pH on Pb adsorption with ASF biomass, (b) adsorbent dose on Pb adsorption with ASF biomass, (c) contact time on Pb adsorption with ASF biomass, (d) initial Pb concentration on Pb adsorption with ASF biomass and (e) agitation speed on Pb adsorption with ASF biomass.

Figure 1 (d) shows the effect of different Pb ion concentrations on the adsorption of Pb on ASF biomass. Adsorption decreased with an increase in initial Pb ion concentration due to the limited available binding sites on the biomass. With a progressive increase in metal ion concentration, the number of available active sites on the biomass for Pb binding were gradually decreased. Jeyakumar and Chandrasekaran [26] found that adsorption efficiency declines with increase in the concentration of Pb ions.

Figure 1(e) depicts the impact of rotation per minute on the adsorption of Pb. Pb adsorption increased with an increase in agitation speed. The highest removal of Pb ions (91.08%) was attained at an agitation speed of 250 rpm and can be attributed to turbulence reduces the boundary layer thickness around the ASF adsorbent particles and favours the increase in Pb adsorption.

The results of our study are in accordance with the earlier studies done on Pb with different adsorbents [27].

Isothermal analysis

An isothermal adsorption study was performed to determine the Pb adsorption capacity of the ASF biomass. Analysis of experimental data with the help of different isotherm models throws light on the nature of metal–biomass interactions, and helps designing an effective operating system. They contribute towards an understanding of the mechanism of sorption and its physicochemical processes. Adsorption isotherms provide the maximum equilibrium sorption capacity of an adsorbent.

The isothermal model parameters are explained in Table 1. The amount of Pb ions adsorbed per unit mass of ASF biomass and the remaining Pb ion concentration (mg L^{-1}) in solution are shown in Figure 2(a), 2(b), and 2(c). The "best fit" was determined by R^2 value and error functions. The R^2 values for Langmuir, Temkin, and Freundlich isotherm models and the values for the error functions (Table 1) reveal that the Freundlich isotherm model had the lowest error function values, and consequently, best fitted the data. Accordingly, the Freundlich isotherm model efficiently explained the present adsorption data com-pared to the other two models. The constant KT represent the binding at equilibrium. It determines the strength of the interaction between the metal and the adsorbent. The greater values of KT suggest stronger adsorption, in this case the adsorption strength was moderate. The Constant 'b' represent the heat of adsorption. The value of b was 597.86 j mol^{-1} which suggests the stronger interaction between the lead ions and the adsorbent but due to the lower value of R^2, Temkin isotherm was not the best-fit model to explain the experimental data. It was found that the Langmuir adsorption capacity (qmax) was 50 mg g^{-1} for Pb ions. In an aqueous solution, the surface area of the biomass plays a vital role in the sorption of metal ions. The sorption capacity of ASF adsorbent for Pb (50 mg g^{-1}) was greater than several other adsorbents, though it was less than that of coconut shell and modified rice husk (Table 2).

The plot acquired from the Scatchard plot analysis in Figure 2(d) was non-linear, suggesting the presence of numerous binding sites on the surface of the biomass.

Kinetic analysis

Kinetic adsorption is a function of the adsorbent-adsorbate reaction and the system in which these are operating. The sorption rate and its mechanism can be investigated through kinetics. Investigation using adsorption kinetics was done so that the uptake rate of Pb by adsorbent could be analysed.

Table 3 presents the data of parameters derived from these linear and non-linear kinetic models. The pseudo-first-order model (Figure 3a) does not adequately fit the adsorption data based on the R^2 values, while the value of R^2 is high for pseudo-second-order kinetics, suggesting that second-order kinetics explains the data of adsorption more accurately (Figures 3b and 3c). Therefore, rate-limiting step is the pseudo-second-order rate kinetics (R^2 =0.999) [28–29].

Table 1 Values of adsorption isothermal constants and the values of error functions

Langmuir		Freundlich		Temkin		D-R isotherm	
q_m(mg g^{-1})	50	K_F(L g^{-1})	8.035	K_T(L g^{-1})	12.554	q_m	0.883
K_L (Lg^{-1})	0.038	1/n	0.302	b($Jmol^{-1}$)	597.86	β	8×10^{-3}
R^2	0.714	R^2	0.826	R^2	0.602	R^2	0.559
RMSE	0.259	RMSE	0.122	RMSE	6.840	RMSE	0.86
EABS	0.112	EABS	0.010	EABS	0.049	EABS	7.212
SD	0.062	SD	0.020	SD	1.82	SD	0.540
χ^2	0.829	χ^2	0.116	χ^2	8.607	χ^2	29.114

Table 2 Comparison of monolayer adsorption capacities of various adsorbent for Pb

Adsorbent	Adsorption capacity (mg g^{-1})	Reference
Rice straw carbon	121.30	[44]
Alstonia scholaris fruit biomass	50	Present study
Algal waste	44	[45]
Tea waste	33.49	[46]
Hazelnut husk (HH)	13.05	[47]
Walnut shell	9.912	[48]
Cedar leaf ash	7.232	[49]
Sawdust	3.19	[50]
Bagasse fly ash	2.50	[51]

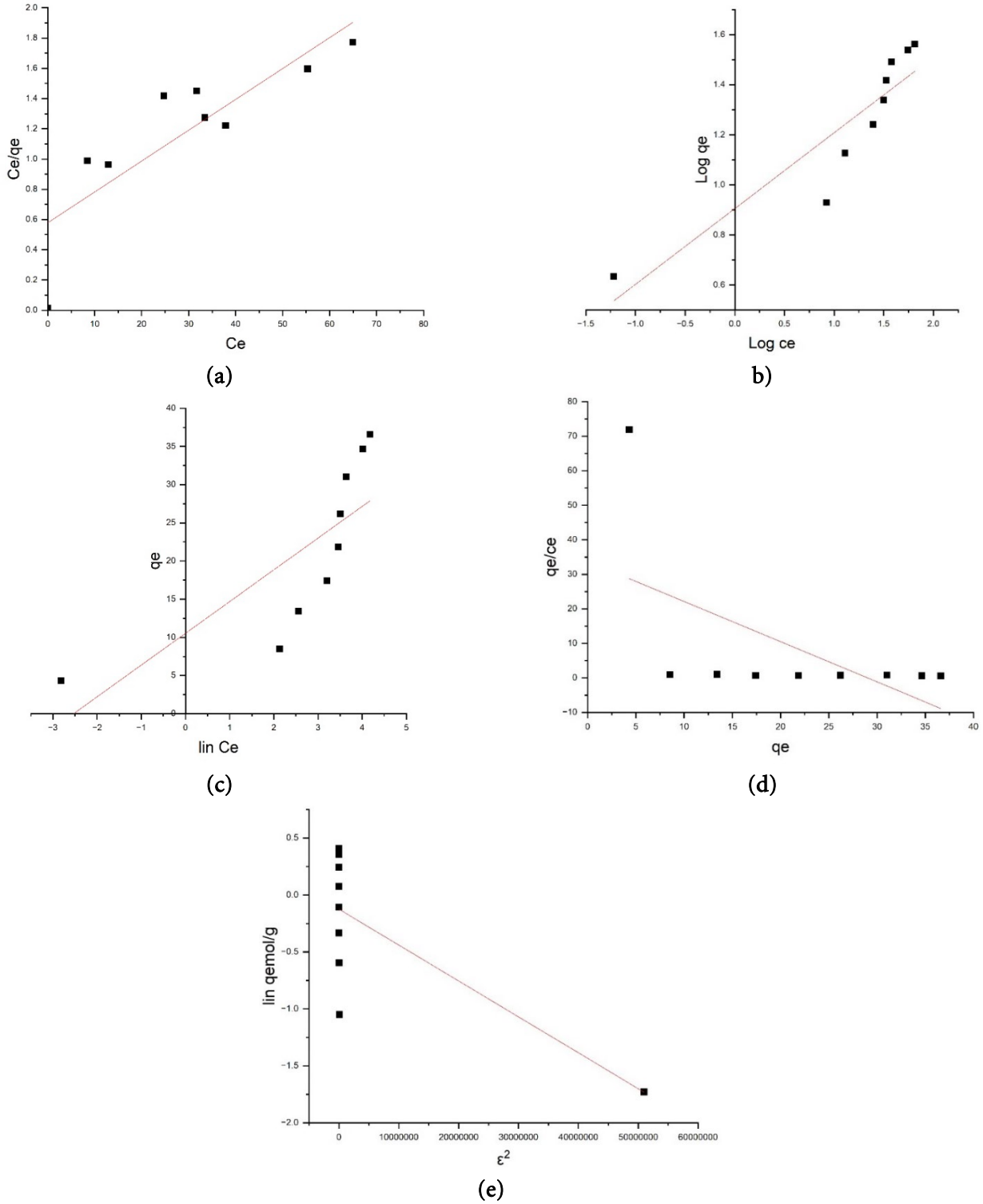

Figure 2 (a) Langmuir isotherm model (b) Freundlich isotherm model (c) Temkin isotherm model (d) Scatchard analysis, of Pb adsorption on ASF biomass (e) D-R isotherm model

Figures 3(d) and 3(e) shows that the curve of the intraparticle diffusion plot was non-linear. Intraparticle diffusion model did not originate from the origin, which indicates that Pb sorption process was not controlled by intraparticle diffusion model [30]. The obtained intraparticular diffusion model constants are depicted in Table 3.

Competitive adsorption

The adsorption efficiency of Pb was investigated in the presence of other metal ions, such as Cd, Zn, and Cu, at pH 5.0. The initial measured concentrations of Pb, Cu, Zn and Cd were 99.9, 99.77, 99.39, and 99.39 mg L^{-1}, respectively. The respective percentage removal of these metal ions was 99.07% (Pb), 92.97 % (Cu), 71.99 % (Zn) and 69.23 % (Cd). The adsorption on

ASF biomass follows the order Pb>Cu>Zn>Cd in a multicomponent system. These findings can be explained on the basis of the physicochemical characteristics of the metal ions. The specificity of the ion exchange in competitive adsorption systems as well as the preference of metal ions on the ASF adsorbent, may be the possible reason for the sorption order of the metal ions. The results may also be explained on the basis of the higher electronegativity of the Pb ion as well as its higher paramagnetic, standard reduction potential, and atomic weight compared to that of the other metal ions used in the experiment. These findings are also supported by earlier works, which found that Pb ions had the highest adsorption in a multimetal medium [31].

Desorption experiment

To determine whether physisorption, ion exchange, or complex formation was the mechanism of Pb adsorption on ASF adsorbent, desorption experiments were conducted. Four eluents: H_2O, 0.1 M NaOH, 0.1 M HNO_3, and 0.1M EDTA were used as desorption media. Desorption with distilled water revealed 0.1% Pb desorption with no impact of time (24 h) suggesting that adsorption of Pb was not through physisorption. Desorption of Pb was 3.54% with NaOH, suggesting a minor role played by chemisorption. On the other hand, desorption with HNO_3 and EDTA yielded 77.04% and 81.00% desorption, respectively. These findings reveal that adsorption of Pb on ASF adsorbent occurred mainly through ion-exchange and complexation mechanisms between the adsorbent and metal ions. It was also suggested that complexation occurs through hydrogen bonding between Pb and the adsorbent, which can be inferred as a nonspecific hydrogen bonding mechanism [32].

Table 3 Kinetic parameters of linear and non-linear pseudo-first-order, pseudo-second-order, and intraparticle diffusion model

Kinetics	Concentration (mg L^{-1})	Parameters	Linear	Non-Linear
Pseudo-first-order model	81.268	q_e (mg g^{-1})	1.4157	7.712
		K_1	1.4×10^{-2}	0.345
		R^2	0.840	0.679
		Chi-square	0.356	0.015
	198.78	q_e (mg g^{-1})	10.889	18.856
		K_1	0.011	0.020
		R^2	0.947	0.907
		Chi-square	2115.57	0.209
Pseudo-second-order model	81.268	q_e (mg g^{-1})	7.937	0.141
		K_2	1.899×10^{-2}	56.050
		R^2	0.999	0.898
		Chi-square	0.011	0.005
	198.78	q_e (mg g^{-1})	20.833	0.039
		K_2	2.047×10^{-3}	518.927
		R^2	0.999	0.989
		Chi-square	127.60	0.023
Intraparticle diffusion model	81.268	C (mg g^{-1})	6.995	6.391
		K_p (mg g^{-1} $min^{-1/2}$)	1.4×10^{-2}	0.321
		R^2	0.811	0.843
		Chi-square	0.006	0.007
	198.78	C (mg g^{-1})	13.28	8.804
		K_p (mg g^{-1} $min^{-1/2}$)	0.312	2.388
		R^2	0.925	0.940
		Chi-square	41.884	0.111

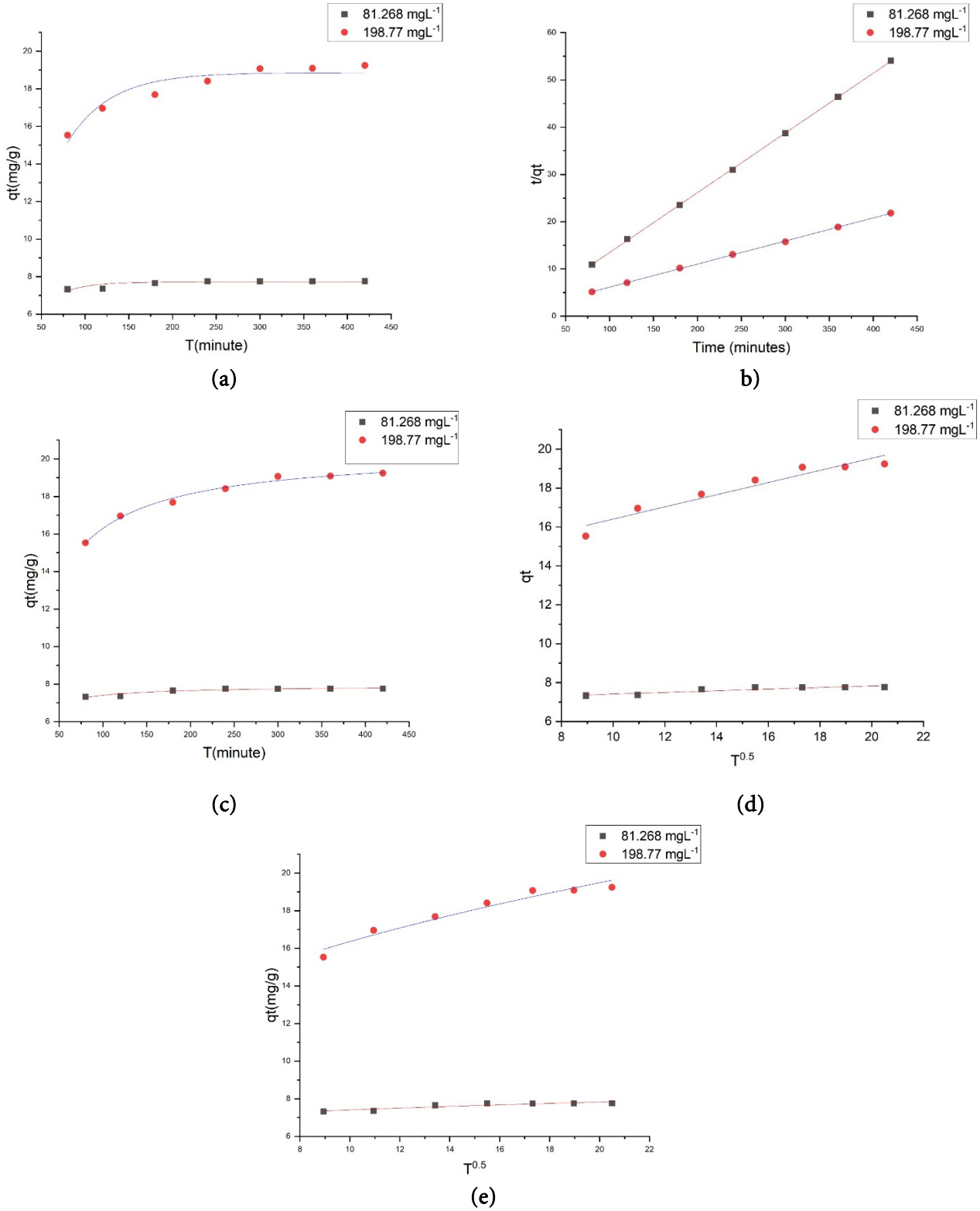

Figure 3 Plots of (a) Non-linear Pseudo-first order kinetics, (b) Linear Pseudo-second order kinetics (c) Non-Linear Pseudo-second order kinetics, (d) Linear Intraparticular diffusion and (e) Non-Linear Intraparticular diffusion model on Pb adsorption by ASF biomass.

Characterisation of the adsorbent

The surface of the adsorbents has an important role to play in the adsorption phenomena. The scanning electron micrographs of the ASF adsorbent before and after the adsorption of Pb are shown in Figures 4 (a) and 4 (b), respectively. Before adsorption, the surface of the ASF adsorbent was found to have a layered structure with irregular protuberances. This irregular surface of the adsorbent facilitated the adsorption of the metal on the adsorbent [33]. After adsorption the adsorbent surface had a more smothered and uniform appearance.

Determination of the surface area was done by BET analysis. The surface area of the ASF adsorbent was 0.23321 $m^2 g^{-1}$, which is low compared to that of coconut shell (0.710 $m^2 g^{-1}$), coco-peat (1.230 $m^2 g^{-1}$) [34] and Cocos nucifera shell (0.4 $m^2 g^{-1}$) [35]. On the other hand, it was higher than that of Moringa oleifera seeds (0.1 $m^2 g^{-1}$) [35].

The impact of chemical treatment on the functional groups of ASF adsorbent was significant when compared to the control. During the carboxylic functional group modification, biosorption of Pb(II) was strongly hindered (19.88% reduction in Pb(II) uptake), highlighting the importance of the carboxylic functional group in Pb(II) uptake on ASF biomass. The impact of methylation of amino acids was approximately a 4.68% reduction in the Pb (II) sorption on the ASF biomass. When data from the control and the chemically modified adsorbents were compared, it was revealed that Pb (II) uptake was more susceptible to carboxyl functional group modification than amine groups. The chemical treatment of the lipids was thought to affect Pb (II) adsorption efficiency, but the findings showed a minor decrease, with only a 2.44 % reduction in the Pb(II) adsorption efficiency occurred with ASF adsorbent (Table 4).

The impact of chemical treatments on the adsorption efficiency of the adsorbents used was found to be biomass-dependent. Despite methylation of functional groups reduced Pb (II) adsorption by 53.38% in biomass of Saccharomyces cerevisiae, the severe reduction drop of 96.34 % was found with esterification of the carboxylic group [37]. According to Kilic et al. [38], the carboxylic functional group was more successful in Pb(II) adsorption, but amine groups were more successful in Hg (II) sequestration.

Moreover, the primary sites of heavy metal accumulation on the surface of Penicillium cyclopium were identified as hydroxyl groups > amides > carboxylates. Lipid and phosphate fractions did not play a significant influence in metal sorption [39]. It can be concluded from the modification of functional groups that Pb(II) binding onto ASF adsorbent also relies on the type of functional group (carboxylic, amine and hydroxyl groups) present on the adsorbent.

Table 4 Reduction in adsorption efficiency after modification of the *Alstonia scholaris* adsorbent

Functional group	Adsorption efficiency (%)	Reduction in adsorption efficiency (%)
Carboxylic group	70.56	19.88
Amine group	85.76	4.68
Lipid group	88.00	2.44
Control	90.44	-

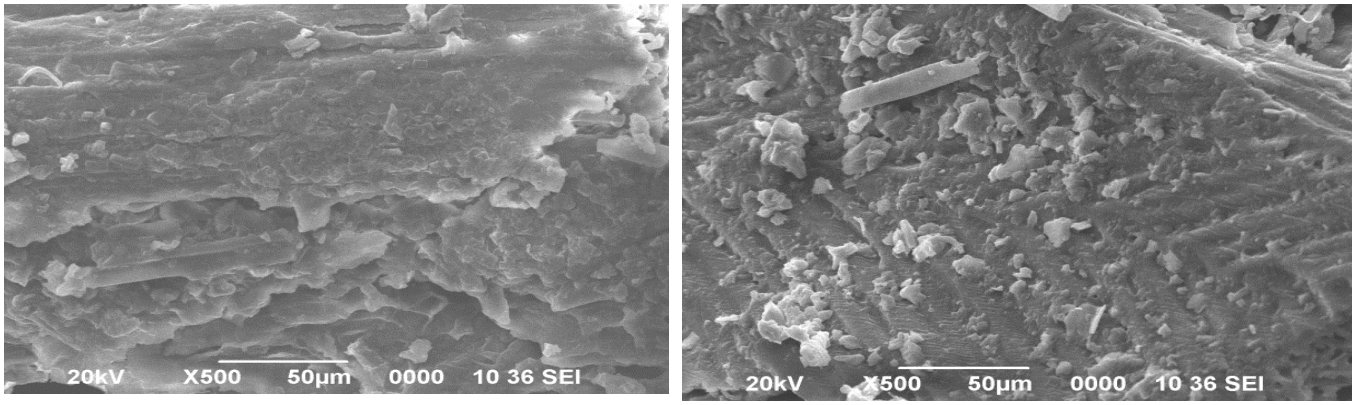

(a) b)

Figure 4 SEM images of ASF biomass (a) before Pb adsorption (b) after Pb adsorption.

Mechanism of adsorption

Evaluation of the mechanism of adsorption was investigated in the present study in order to know the specific cause of binding on the adsorbent molecules. Based on the isothermal analysis of the study, Freundlich isotherm explained the study best fit, which supports chemisorption mechanism of the adsorption process. Though the D-R isotherm (Figure 2e) did not give the best fit for the data it threw light on the mechanism of adsorption. It is known that if the free energy value 'E' is less than 8 kJ mol^{-1} it means that adsorption followed physical mechanism, whereas if it is between 8–16 kJ mol^{-1}, adsorption comprised chemisorption. The value of free energy of D-R isotherm in the present study was less than 8 kJ mol^{-1} indicating that physical adsorption also played a role in the adsorption of Pb on ASF biomass.

Similarly, kinetic analysis showed that pseudo second order kinetic model best explained the data of the study, which suggests that adsorption occurred through

chemisorption or chemical mechanism. Scatchard plot was not linear as shown in Figure 2(d) which also suggests that the presence of numerous binding sites on the adsorbent. The chemical modification of functional groups revealed that the functional groups of ASF adsorbent especially carboxylic acid and amines took part in the adsorption of Pb. Desorption analysis showed that EDTA, HNO_3 and NaOH could desorb Pb from the adsorbent. The findings obtained from the desorption analysis shows that adsorption occurring with EDTA was corresponding with complexation, that with HNO_3 to ion-exchange, and with NaOH corresponding to chemisorption mechanisms.

To conclude, the mechanism of the present adsorption study was complex which means that adsorption involved more than one mechanism simultaneously. The findings of this study are supported by that of Jin and Bai [40] that Pb adsorption followed ion-exchange, complexation and physical mechanism on Chitosan/PVA hydrogel beads. Similarly, Eick et al. [41], and Chen et al. [42] also found that Pb adsorption mechanism was complex in nature. All these studies lend support to our contention that Pb adsorption on ASF biomass was complex in nature.

Reusability of ASF biomass

The regeneration capacity is one of the most important characteristics of an adsorbent, which enables an adsorbent to be used successively for the removal of heavy metals in different adsorption cycles. The reusability potential of ASF biomass was assessed by desorption experiment using EDTA as eluent. Adsorption-desorption cycles were performed up to 50% reduction in the adsorption efficiency of the adsorbent. Consecutive loss in adsorption efficiency from cycle to cycle was observed (Figure 5). There was a decrease in adsorption efficiency, which could be attributed to the structural deformation of the sorbent caused by extended shaking during the adsorption–desorption cycles [43].

Conclusions

It has been concluded that ASF biomass may be considered as an alternative option for removing Pb from wastewater. The study elucidated the multifaceted dynamics of Pb adsorption onto ASF biomass, shedding light on pivotal factors influencing the process. The pH was found to significantly impact adsorption efficiency, with an optimum pH of 5 facilitating maximal Pb adsorption due to the adsorbent surface's negative charge and subsequent ion binding. Similarly, the adsorbent dose played a critical role, with an increase up to 2.50 g per 100 mL enhancing adsorption efficiency before diminishing returns were observed. Contact time also proved influential, reaching peak adsorption efficiency at 420 min. Moreover, initial Pb concentration negatively correlated with adsorption, emphasizing the saturation of available binding sites with increasing metal ion concentration. The isothermal interpretations showed the maximum adsorption capacity was 50 mg g^{-1} which compares well with several adsorbents and the optimum removal percentage was 97%. The Freundlich isotherm model explained the sorption process efficiently. Scatchard analysis indicated the presence of multiple binding spots on the ASF biomass surface. The best fit was depicted by pseudo-second-order kinetics. SEM and chemical modification of the adsorbent revealed the participation of functional groups - mainly carboxyl - in the adsorption process. EDTA was found to be the best eluent for desorption of Pb from ASF biomass. Multi-metal adsorption studies revealed Pb>Cu>Zn>Cd adsorption order. These findings deepen our understanding of Pb adsorption onto ASF biomass, offering insights into optimizing adsorption processes for lead removal from wastewater.

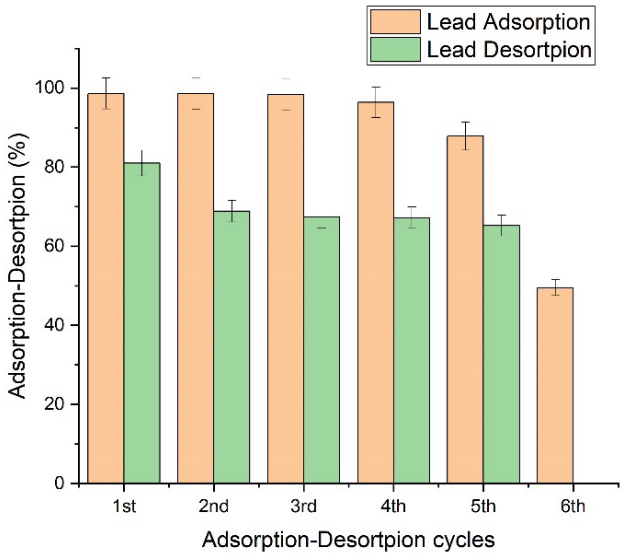

Figure 5 Regeneration of the ASF biomass.

References

[1] El-Azazy, M., El-Shafie, A.S., Issa, A.A., Al-Sulaiti, M., AL-Yafie, J., Shomar, B., Al-Saad, K. Potato peels an adsorbent for heavy metals from aqueous solutions: Eco- structuring of a green adsorbent operating Plackett- Burma design. Journal of Chemistry, 2019, 14.

[2] Boudrahem, F., Aissani-Benissad, F., Soualah, A. Adsorption of lead(II) from aqueous solution by using leaves of date trees as an adsorbent. Journal of Chemical Engineering Data, 2011, 56, 1804–1812.

[3] Demirbas, A. Heavy metal adsorption onto agro-based waste materials: A review. Journal of Hazardous Materials, 2008, 157, 220–229.

[4] Shankar, S., Joshi, S., Srivastava, R.K. A review on heavy metal biosorption utilising modified chitosan. Environmental Monitoring and Assessment, 2023, 195, 1350

[5] Ahluwalia, S.S., Goyal, D. Removal of heavy metals by waste tea leaves from aqueous solution. Engineering in Life Sciences. 2005, 5, 158–162.

[6] Tejada-Tovar, C., Gonzalez-Delgado, A.D., Villabona-Ortiz, A. Characterisation of residual biomasses and its application for the removal of lead ions from aqueous solution. Applied Sciences, 2019, 9, 4486.

[7] Yang, Y., Jin, D., Wang, G., Liu, D., Jia, X., Zhao, Y. Biosorption of Acid Blue 25 by unmodified and CPC-modified biomass of Penicillium YW01: Kinetic study, equilibrium isotherm and FTIR analysis. Colloids and Surfaces B: Biointerfaces, 2011, 88, 521–526.

[8] Kapoor, A., Viraraghavan, T. Heavy metal biosorption sites in Aspergillus niger. Bioresource Technology, 1997, 61, 221–227.

[9] Kilic, M., Keskin, M.E, Mazlum, S., Mazlum, N. Hg (II) and Pb (II) adsorption on activated sludge biomass: Effective biosorption mechanism. International Journal of Mineral Processing, 2008, 87, 1–8.

[10] Tobin, J.M., Cooper, D.G., Neufeld, R.J. Investigation of the mechanism of metal uptake by denatured Rhizopus arrhizus biomass. Enzyme and Microbal Technology, 1990, 12, 591–595.

[11] Lukman, S., Essa, M. H., Dalhat, N., Basheer, C. Adsorption and desorption of heavy metals onto natural clay material: Influence of initial pH. Journal of Environmental Science and Technology, 2013, 6, 1–15.

[12] Moghal, A.A. B., Al-Shamrani, M.A., Zahid, W. M. Heavy metal desorption studies on the artificially contaminated Al-Qatif soil. International Journal of GEOMATE, 2015, 8, 1323–1327.

[13] Liu, R., Guan, Y., Chen, L., Lian, B. Adsorption and desorption characteristics of Cd^{2+} and Pb^{2+} by micro and nano-sized biogenic $CaCO_3$. Frontiers in Microbiology, 2018, 9, 41.

[14] D browski, A. Adsorption — From theory to practice. Advances in Colloid and Interface Science, 2001, 93(1–3), 135–224.

[15] He, Y., Wu, P., Xiao, W., Li, G., Yi, J., He, Y., … Duan, Y. Efficient removal of Pb (II) from aqueous solution by a novel ion imprinted magnetic biosorbent: Adsorption kinetics and mechanisms. PLos One, 2019, 14, e0213377.

[16] Ayawei, N., Ebelegi, A.N., Wankasi, D. Modelling and interpretation of adsorption isotherms. Journal of Chemistry, 11.

[17] Qi, J., Li, Y., Majeed, H., Goff, H.D., Rahman, M.R.T., Zhong, F. Adsorption mechanism modelling using lead (Pb) sorption data on modified rice bran-insoluble fibre as universal approach to assess other metals toxicity. International Journal of Food Properties, 2019, 22, 1397–1410.

[18] Bairagi, H., Khan, M.M.R, Ray, L., Guha, A.K. Adsorption profile of lead on Aspergillus versicolor: A mechanistic probing. Journal of Hazardous Materials, 2011, 186, 756–764.

[19] Colak, F., Atar, N., Olgun, A. Biosorption of acidic dyes from aqueous solution by Paenibacillus macerans: Kinetic, thermos-dynamic and equilibrium studies. Chemical Engineering Journal, 2009, 150, 122–130.

[20] Balarak, D., Salari, A.A. Error analysis of adsorption isotherm models for sulfamethazine onto multi walled carbon nanotubes. Journal of Pharmaceutical Research International, 2019, 25, 1–10.

[21] Prasad, A.L., Santhi, T., Manonmani, S. Recent developments in preparation of activated carbons by microwave: Study of residual errors. Arab Journal of Chemistry, 2015, 8, 343 –354.

[22] Tsai, S.C., Juang, K.W. Comparison of linear and nonlinear forms of isotherm models for strontium sorption on a sodium bentonite. Journal of Radioanalytical and Nuclear Chemistry, 2000, 243, 741–746.

[23] Ho, Y.S. Effect of pH on lead removal from water using tree fern as the sorbent. Bioresource Technology, 2005, 96, 1292–1296.

[24] Amini, M., Younesi, H., Bahramifar, N., Lorestani, A.A.Z., Ghorbani, F., Daneshi, A., Sharifzadeh, M. Application of response surface methodology for optimisation of lead biosorption in an aqueous solution by Aspergillus niger. Journal of Hazardous Materials, 2008, 154, 694–702.

[25] Farghali, A.A., Bahgat, M., Enaiet Allah, A., Khedr, M.H. Adsorption of Pb (II) ions from aqueous solutions using copper oxide nanostructures. Beni-Suef University Journal of Basic and Applied Sciences, 2013, 2, 61–71.

[26] Jeyakumar, R.P.S., Chandrasekaran, V. Adsorption of lead (II) ions by activated carbons prepared from marine green algae: equilibrium and kinetics studies. International Journal of Industrial Chemistry, 2014, 5, 1–9.

[27] Al-Qodah, Z. Adsorption of dyes using shale oil ash. Water Research, 2000, 34, 4295–4303.

[28] Aroua, M.K., Lepmg, S.P.P, Teo, L.Y., Yin, C.Y., Daud, W.M.A.W. Real-time determination of kinetics of adsorption of lead(II) onto palm shell-based activated carbon using selective electrode. Bioresource Technology, 2008, 99, 5786–5792.

[29] Mohanty, K., Naidu, J.T., Meikap, B.C., Biswas, M.N. Removal of crystal violet from wastewater by activated carbons prepared from rice husk. Industrial & Engineering Chemistry Research, 2006, 45, 5165–5171.

[30] Radhika, M., Palanivelu, K. Adsorptive removal of chlorophenols from aqueous solution by low cost adsorbent-kinetics and isotherm analysis. Journal of Hazardous Materials, 2006, 138, 116–124.

[31] Sahmoune, M.N., Louhab, K., Boukhiar, A., Addad, J., Barr, S. Kinetic and equilibrium models for the biosorption of Cr(III) on Streptomyces rimosus. Toxicological & Environmental Chemistry, 2009, 91, 1291–1303.

[32] Mohan, S.V., Karthikeyan, J. Adsorptive removal of reactive azo dye from an aqueous phase onto charfines and activated carbon. Clean Technologies and Environmental Policy, 2004, 6, 196–200.

[33] Bradl, H. B. Adsorption of heavy metal ions on soils and soils constituents. Journal of Colloid and Interface Science, 2004, 277(1), 1-18.

[34] Hetttiarachchi, E., Perera, R., Chandani Perera, A.D.L., Kottegoda, N. Activated coconut coir for removal of sodium and magnesium ions from saline water. Desalination and Water Treatment, 2016, 22341–22352.

[35] Acheampong, M.A., Ansa, E.D.O., Woode, M.Y., Awuah, E. Biosorption of Pb(II) onto Cocos nucifera shell and Moringa oleifera seeds. Chemical Engineering Communications, 2015, 202, 946–953.

[36] Gaur, N., Kukreja, A., Yadav, M., Tiwari, A. Adsorptive removal of lead and arsenic from aqueous solution using soya bean as a novel biosorbent: equilibrium isotherm and thermal stability studies. Applied Water Science, 2018, 8(98).

[37] Jianlong, W. Biosorption of copper(II) by chemically modified biomass of Saccharomyces cerevisiae. Process Biochemistry, 2002, 37(8), 847–850.

[38] Kilic, M., Keskin, M. E., Mazlum, S., Mazlum, N. Hg(II) and Pb(II) adsorption on activated sludge biomass: Effective biosorption mechanism. International Journal of Mineral Processing, 2008, 87, 1–8.

[39] Tsekova, K., Christova, D., Ianis, M. Heavy metal biosorption sites in Penicillium cyclopium. Journal of Applied Sciences and Environ-mental Management, 2006, 10, 117–121.

[40] Jin, L., Bai, R. Mechanisms of lead adsorption on chitosan/PVA hydrogel beads. Langmuir, 2002, 18, 9765–9770.

[41] Ozacar, M., Sengil, I.A, Terkmenler, H. Equilibrium and kinetic data, and adsorption mechanism for adsorption of lead onto valonia tannin resin. Chemical Engineering Journal, 2008, 143, 3242.

[42] Chen, C., Chen, Q., Kang, J., Shen, J., Wang, B., Guo, F., Chen, Z. Hydrophilic triazine-based dendron for copper and lead adsorption in aqueous systems: Performance and mechanism. Journal of Molecular Liquids, 2020, 298, 112031.

[43] Saeed, A., Iqbal, M. Bioremoval of cadmium from aqueous solution by black gram husk (Cicer arientinum). Water Research, 2003, 37(14), 3472–3480.

[44] Qiu, Y., Cheng, H., Xu, C., Sheng, G. D. Surface characteristics of crop-residue-derived black carbon and lead(II) adsorption. Water Research, 2008, 42(3), 567–574.

[45] Vilar, V.J.P., Botelho, C.M.S, Martins, R.J.E., Boaventura, R.A.R. Continuous biosorption of single and binary metal solutions in a fixed-bed column using algae and granulated algal waste from agar extraction. Water Resources Research Progress, 2008, 275–296.

[46] Wan, S., Ma, Z., Xue, Y., Ma, M., Xu, S., Qian, L., Zhang, Q. Sorption of lead(II), cadmium(II), and copper(II) ions from aqueous solutions using tea waste. Industrial & Engineering Chemistry Research, 2014, 53, 3629–3635.

[47] Imamoglu, M., Tekir, O. Removal of copper (II) and lead(II) ions from aqueous solutions by adsorption on activated carbon from a new precursor hazelnut husks. Desalination, 2008, 228, 108–113.

[48] Celebi, H., Gok, O. Evaluation of lead adsorption kinetics and isotherms from aqueous solution using natural walnut shell. International Journal of Environmental Research, 2017, 11, 83–90.

[49] Hafshejani, L.D., Nasab, S.B., Gholami, R.M., Moradzadeh, M., Izadpanah, Z., Hafshejani, S.B., Bhatnagar, A. Removal of zinc and lead from aqueous solution by nanostructured cedar leaf

ash as biosorbent. Journal of Molecular Liquids, 2015, 211, 448–456.

[50] Yu, B., Zhang, Y., Shukla, A., Shukla, S.S., Dorris, K.L. The removal of heavy metals from aqueous solutions by sawdust adsorption — Removal of lead and comparison of its adsorption with copper. Journal of Hazardous Materials, 2001, 84(1), 83–94.

[51] Gupta, V.K., Ali, I. Removal of lead and chromium from wastewater using bagasse fly ash-a sugar industry waste. Journal of Colloid and Interface Science, 2004, 271, 321–328.